

# Nonequilibrium Green's function method for phonon-phonon interactions and ballistic-diffusive thermal transport

Yong Xu,<sup>1,2</sup> Jian-Sheng Wang,<sup>2</sup> Wenhui Duan,<sup>1,\*</sup> Bing-Lin Gu,<sup>1</sup> and Baowen Li<sup>2,3</sup>

<sup>1</sup>Center for Advanced Study and Department of Physics, Tsinghua University, Beijing 100084, China

<sup>2</sup>Department of Physics and Centre for Computational Science and Engineering, National University of Singapore, Singapore 117542, Republic of Singapore

<sup>3</sup>NUS Graduate School for Integrative Sciences and Engineering, Singapore 117597, Republic of Singapore

(Received 24 July 2008; revised manuscript received 13 October 2008; published 4 December 2008)

Phonon-phonon interactions are systematically studied by nonequilibrium Green's function (NEGF) formalism in momentum space at finite temperatures. Within the quasiparticle approximation, phonon frequency shift and lifetime are obtained from the retarded self-energy. The lowest-order NEGF provides the same phonon lifetime as Fermi's golden rule. Thermal conductance is predicted by the Landauer formula with a phenomenological transmission function. The main advantage of our method is that it covers both ballistic and diffusive limits, and thermal conductance of different system sizes can be easily obtained once the mode-dependent phonon mean-free path is calculated by NEGF. As an illustration, the method is applied to two one-dimensional atom chain models [the Fermi-Pasta-Ulam (FPU)- $\beta$  model and the  $\phi^4$  model] with an additional harmonic on-site potential. The obtained thermal conductance is compared with that from a quasiclassical molecular-dynamics method. The harmonic on-site potential is shown to remove the divergence of thermal conductivity in the FPU- $\beta$  model.

DOI: [10.1103/PhysRevB.78.224303](https://doi.org/10.1103/PhysRevB.78.224303)

PACS number(s): 63.20.kg, 63.22.-m, 66.10.cd, 44.10.+i

## I. INTRODUCTION

More understanding of nanoscale thermal transport is required to solve heat dissipation problem, which becomes important as the size of electronic device decreases.<sup>1</sup> In recent years, many experiments have been done to measure thermal conduction of nanostructures.<sup>2-5</sup> At the nanoscale, the ballistic approximation is usually a good starting point for thermal transport and a lot of theoretical research on ballistic thermal transport have been reported.<sup>6-9</sup> However, the ballistic approximation would lead to unphysical results, such as infinite phonon mean-free path, divergent thermal conductivity, and zero-temperature gradient. In most cases we need to go beyond ballistic limit to include effects of scattering for a more realistic consideration. In fact, phonon-phonon interaction is one of the significant factors for understanding and improving thermal transport properties. Since the sizes of nanostructures are comparable to phonon mean-free path, thermal transport in these systems is in the intermediate region between ballistic and diffusive ranges. Nanoscale thermal transport has been studied through many approaches.<sup>10-22</sup> Nevertheless, no satisfactory method has been available to deal with thermal transport in the intermediate region.

Our work aims to provide an efficient way to study ballistic-diffusive thermal transport including the effects of phonon-phonon interactions. Here we propose a formalism of nonequilibrium Green's function (NEGF) to treat phonon-phonon interactions in momentum space at finite temperatures. It is known that NEGF is usually used to study nonequilibrium problems but its formalism can be applied to equilibrium systems as well. While the Matsubara formalism<sup>23</sup> is conventionally used for equilibrium Green's function calculation at finite temperatures, NEGF is an alternative that also works for such situations. NEGF has advantage over the Matsubara formalism in the numerical calculation

of phonon lifetime when high order perturbations are considered. In our framework of NEGF, the analytical form of phonon self-energy to any order can be easily derived and phonon frequency shift and lifetime are directly related to the retarded self-energy. The phonon frequency shift can also be accurately predicted by an effective phonon theory based on the ergodic hypothesis (equipartition theorem).<sup>24-26</sup> For weak phonon-phonon interactions, however, frequency shift is usually very small and the major influence on thermal transport is from the finite phonon lifetime. It will be shown that NEGF of lowest order is equivalent to Fermi's golden rule when considering phonon lifetime.

We also provide an approach in studying thermal transport using NEGF. Our NEGF formalism gives phonon lifetime and mean-free path. Using a phenomenological transmission function determined from mean-free path in the Landauer formula, ballistic-diffusive thermal transport can be studied.<sup>10,27,28</sup> Many works have been done on thermal transport by NEGF.<sup>18-22</sup> In previous treatments, the system is situated at the center as a junction with semi-infinite leads on the two sides. The central part cannot be too large due to the constraint of computational capability. Here we compute phonon lifetime in a periodic system at equilibrium, and feed the lifetime information to phonon transmission function in the Landauer formula. Our approach is computationally more efficient but with a less rigorous treatment of transmission function.

In Sec. II, the general theory of NEGF is developed for phonon-phonon interactions and ballistic-diffusive thermal transport. As an application we employ the method to study two explicit models in Sec. III. A summary is made in Sec. IV.

## II. GENERAL THEORY

In the harmonic approximation, a crystal can be described in terms of noninteracting phonons. The concept of "pho-

non" remains valid when the anharmonic contribution is small compared with the harmonic. In this case, the quasiparticle approximation can be made, and then the anharmonic effects give a complex shift to phonon frequency:<sup>29</sup> the real part shifts the value of frequency while the imaginary part corresponds to phonon lifetime.

One of the earliest methods<sup>30–32</sup> of calculating phonon lifetime is based on Fermi's golden rule and the Boltzmann-Peierls equation. However, those approaches cannot be systematically improved. In contrast, the Green's function method provides a systematic way in considering phonon-phonon interactions at finite temperatures. Phonon-phonon interactions have been studied using equilibrium Green's function method.<sup>29,33–37</sup> These works can be roughly divided into two groups according to the decoupling schemes used. For the first group, the temperature-dependent Green's function with Matsubara representation is employed based on a general Wick's theorem which holds when the system is large enough.<sup>29,33–35</sup> A fictitious imaginary time is used and an analytical continuation is needed to get the retarded Green's function.<sup>38</sup> For the other group, a decoupling scheme proposed by Procacci and co-workers<sup>36,37</sup> is used. In detail, in the equation of motion for the real time Green's function, thermal averages are replaced with those appropriate for the harmonic Hamiltonian. The analytical expression of phonon self-energy including high order terms can be easily evaluated by a computer-aided technique, despite the lack of a clear theoretical foundation.

We will employ the NEGF method as described in Ref. 39. Its formalism has been generalized to treat arbitrary non-equilibrium systems with arbitrary initial density matrices by Wagner.<sup>40</sup> If interactions are adiabatically switched on and an initial noninteracting Hamiltonian is used, Wick's theorem is still valid for the contour ordered Green's function.<sup>41</sup> The adiabatic switch-on assumption leads to a loss of information related to initial correlation but is still reasonable in most physical situations. We will use this assumption and take the contour ordered Green's function to study phonon-phonon interactions.

In this section, we developed the general theory of NEGF to deal with phonon-phonon interactions and ballistic-diffusive thermal transport. At first, a general Hamiltonian of anharmonic system is given, and the contour ordered Green's function of phonon is defined. Then, two schemes are provided to solve Green's function. One is to use the equation of motion and recursive expansion rules. The other is to apply Feynman rules for self-energy and solve the Dyson equation. Within the quasiparticle approximation, the retarded self-energy directly corresponds to phonon lifetime. Next we will compare the NEGF method with Fermi's golden rule. Finally, we discuss how to study ballistic-diffusive thermal transport with the information of phonon mean-free path.

### A. Hamiltonian

In a Taylor expansion of the potential energy  $\Phi$  at equilibrium configuration, terms higher than the second order constitute anharmonic Hamiltonian:

$$H_A = \sum_{n=3,4,\dots} \frac{1}{n!} \sum_{i_1, i_2, \dots, i_n} \Phi_{i_1 i_2 \dots i_n} u_{i_1} u_{i_2} \dots u_{i_n}. \quad (1)$$

Herein, the system has  $N$  unit cells and each cell contains  $r$  atoms. We use  $i \equiv (n_i, \tilde{i})$  ( $n_i = 1, 2, \dots, N$ ) and  $\tilde{i} \equiv (\kappa_i, \alpha_i)$  ( $\kappa_i = 1, 2, \dots, r$ ;  $\alpha_i = x, y, z$ ) for convenience.  $u_i = \sqrt{M_{\kappa_i}} x_i$ ,  $M_{\kappa_i}$  is the atom mass and  $x_i$  is the displacement. We expand  $u_i$  as

$$u_i = \sum_q \frac{e^{i\mathbf{q}\cdot\mathbf{R}_{n_i}}}{\sqrt{N}} \epsilon_i^j(\mathbf{q}) A_q, \quad q \equiv (\mathbf{q}, j_q), \quad (2)$$

where  $j_q = 1, 2, \dots, 3r$  denotes the phonon branch, and  $\epsilon_i^j(\mathbf{q})$  is the normal-mode eigenvector. The phonon operator  $A_q$  can be expressed by the usual phonon annihilation operator  $a_q$  and creation operator  $a_q^\dagger$ . Introducing  $\bar{q} \equiv (-\mathbf{q}, j_q)$ , we have

$$A_q = \sqrt{\frac{\hbar}{2\omega_q}} (a_q + a_{\bar{q}}^\dagger), \quad A_{\bar{q}}^\dagger = A_q, \quad (3)$$

where  $\omega_q$  is the frequency of the normal mode  $q$ . Then the harmonic Hamiltonian has the form

$$H_0 = \sum_q \frac{1}{2} \dot{A}_q \dot{A}_q + \sum_q \frac{1}{2} \omega_q^2 A_q A_q, \quad (4)$$

$$\dot{A}_q = -i \sqrt{\frac{\hbar\omega_q}{2}} (a_q - a_{\bar{q}}^\dagger). \quad (5)$$

The anharmonic Hamiltonian becomes

$$H_A = \sum_{n=3,4,\dots} \frac{1}{n!} \sum_{q_1, q_2, \dots, q_n} F_{q_1 q_2 \dots q_n} A_{q_1} A_{q_2} \dots A_{q_n}, \quad (6)$$

where the  $n$ -leg vertex is

$$\begin{aligned} F_{q_1 q_2 \dots q_n} &= \frac{\Delta(\mathbf{q}_1 + \mathbf{q}_2 + \dots + \mathbf{q}_n)}{(n-1)! N^{n/2-1}} \\ &\times \sum_{\tilde{i}_1} \sum_{i_2, \dots, i_n} \Phi_{i_1 i_2 \dots i_n} e^{i\mathbf{q}_2 \cdot (\mathbf{R}_{n_{i_2}} - \mathbf{R}_{n_{i_1}})} \dots \\ &\times e^{i\mathbf{q}_n \cdot (\mathbf{R}_{n_{i_n}} - \mathbf{R}_{n_{i_1}})} \times \epsilon_{i_1}^{j_{q_1}}(\mathbf{q}_1) \epsilon_{i_2}^{j_{q_2}}(\mathbf{q}_2) \dots \epsilon_{i_n}^{j_{q_n}}(\mathbf{q}_n). \end{aligned} \quad (7)$$

$\Delta(\mathbf{q}) = 1$  if  $\mathbf{q}$  is zero or a reciprocal-lattice vector; otherwise  $\Delta(\mathbf{q}) = 0$ .

### B. Nonequilibrium Green's function

We define the contour ordered Green's function of phonon as

$$G_{qq'}(\tau, \tau') = -\frac{i}{\hbar} \langle \mathcal{T}_\tau A_q(\tau) A_{q'}(\tau') \rangle, \quad (8)$$

where  $\tau$  and  $\tau'$  are defined in the complex plane,  $\langle \dots \rangle$  denotes the ordinary Gibbs statistical average, and  $\mathcal{T}_\tau$  is the contour-ordering operator. The contour runs slightly above the real axis from  $-\infty$  to  $+\infty$ , and back to  $-\infty$  slightly below the real axis. From our definition, we have

$$G_{qq'}(\tau, \tau') = \delta_{q, \bar{q}'} G_{q\bar{q}}(\tau, \tau'). \quad (9)$$

Note that only those Green's functions of the form  $G_{q\bar{q}}(\tau, \tau')$  are nonzero because of the orthogonality between the normal modes.

The mapping of the contour ordered Green's function onto four different normal Green's functions has been discussed.<sup>10,22,39</sup> A label  $\sigma = \pm 1$  is needed to distinguish whether  $\tau$  is on the upper branch or on the lower branch,

$$G_{qq'}^{\sigma\sigma'}(t, t') = \lim_{\epsilon \rightarrow 0^+} G_{qq'}(t + i\epsilon\sigma, t' + i\epsilon\sigma'). \quad (10)$$

$G^{++} = G^t$ ,  $G^{--} = G^{\bar{t}}$ ,  $G^{+-} = G^<$ , and  $G^{-+} = G^>$ . There are another two types of Green's functions:  $G^r$  and  $G^a$ . The relations among these six Green's functions in time and frequency domains have been presented in Ref. 22.

### C. Equation of motion

Simple recursive expansion rules for the contour ordered Green's function of phonon in coordinate space is originally proposed in Ref. 22. Differently, the phonon operators  $A_q$  used here are not Hermitian. However, we can show that the same recursive expansion rules can be used by our phonon Green's function defined in momentum space.

We define a general  $n$ -point Green's function

$$G_{q_1 q_2 \dots q_n}(\tau_1, \tau_2, \dots, \tau_n) = -\frac{i}{\hbar} \langle T_{\tau} A_{q_1}(\tau_1) A_{q_2}(\tau_2) \dots A_{q_n}(\tau_n) \rangle. \quad (11)$$

The phonon operators satisfy

$$\begin{aligned} \ddot{A}_q &= -\frac{i}{\hbar} [\dot{A}_q, H] = -w_q^2 A_q \\ &- \sum_{n=3,4,\dots} \sum_{q_2, q_3, \dots, q_n} F_{\bar{q} q_2 q_3 \dots q_n} A_{q_2} A_{q_3} \dots A_{q_n}. \end{aligned} \quad (12)$$

From the definition,

$$\begin{aligned} F_{q_1 q_2 \dots q_n}(\tau_1, \tau_2, \dots, \tau_n) &= F_{q_1 q_2 \dots q_n} \delta_{\sigma_1, \sigma_2} \delta(t_1 - t_2) \dots \delta_{\sigma_1, \sigma_n} \\ &\times \delta(t_1 - t_n) \sigma_1^{n-1}. \end{aligned} \quad (13)$$

The equation for the contour ordered Green's function is

$$\begin{aligned} \frac{\partial^2}{\partial \tau^2} G_{qq'}(\tau, \tau') &= -\delta_{q, \bar{q}'} \delta(\tau - \tau') - w_q^2 G_{q, q'}(\tau, \tau') \\ &- \sum_{n=3,4,\dots} \sum_{q_2, \dots, q_n} \int \dots \int d\tau_2 \dots d\tau_n \\ &\times F_{\bar{q} q_2 \dots q_n}(\tau, \tau_2, \dots, \tau_n) G_{q_2 \dots q_n q'} \\ &\times (\tau_2, \dots, \tau_n, \tau'). \end{aligned} \quad (14)$$

The equation for the unperturbed Green's function is

$$\frac{\partial^2}{\partial \tau'^2} G_{qq'}^0(\tau, \tau') = -\delta_{q, \bar{q}'} \delta(\tau - \tau') - w_q^2 G_{qq'}^0(\tau, \tau'). \quad (15)$$

Combining Eqs. (14) and (15), the two-point Green's function can be expressed in terms of the free and higher order ones as

$$G_{qq'}(\tau, \tau') = G_{qq'}^0(\tau, \tau') + \sum_{n=3,4,\dots} \sum_{q_1, q_2, \dots, q_n} \left[ \int \int \dots \int d\tau_1 d\tau_2 \dots d\tau_n G_{qq_1}^0(\tau, \tau_1) F_{q_1 q_2 \dots q_n}(\tau_1, \tau_2, \dots, \tau_n) G_{q_2 \dots q_n q'}(\tau_2, \dots, \tau_n, \tau') \right]. \quad (16)$$

Repeating the above procedures, we can get the equation for higher order Green's functions,

$$\begin{aligned} G_{q_1 q_2 \dots q_n}(\tau_1, \tau_2, \dots, \tau_n) &= i\hbar G_{q_1 q_2}^0(\tau_1, \tau_2) G_{q_3 q_4 \dots q_n}(\tau_3, \tau_4, \dots, \tau_n) + i\hbar G_{q_1 q_3}^0(\tau_1, \tau_3) G_{q_2 q_4 \dots q_n}(\tau_2, \tau_4, \dots, \tau_n) + \dots \\ &+ i\hbar G_{q_1 q_n}^0(\tau_1, \tau_n) G_{q_2 q_3 \dots q_{n-1}}(\tau_2, \tau_3, \dots, \tau_{n-1}) + \sum_{m=3,4,\dots} \sum_{q'_1, q'_2, \dots, q'_m} \\ &\times \left[ \int \int \dots \int d\tau'_1 d\tau'_2 \dots d\tau'_m G_{q_1 q'_1}^0(\tau_1, \tau'_1) F_{q'_1 q'_2 \dots q'_m}(\tau'_1, \tau'_2, \dots, \tau'_m) G_{q'_2 \dots q'_m q_2 \dots q_n}(\tau'_2, \dots, \tau'_m, \tau_2, \dots, \tau_n) \right]. \end{aligned} \quad (17)$$

Equations (16) and (17) are the equations of motion for the contour ordered Green's function, which have the same form as those in Ref. 22. As such, the same recursive expansion rules can be used here. One may conveniently implement these rules in a computer program and expand the Green's function to any order as one wish.

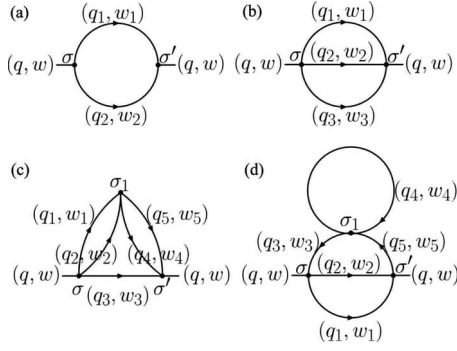


FIG. 1. Feynman diagrams for phonon self-energy.

#### D. Feynman rules for self-energy

The Dyson equation for our Green's function is

$$G_{q\bar{q}}(\tau, \tau') = G_{q\bar{q}}^0(\tau, \tau') + \int \int d\tau_1 d\tau_2 G_{q\bar{q}}^0(\tau, \tau_1) \Sigma_{\bar{q}\bar{q}}(\tau_1, \tau_2) G_{q\bar{q}}(\tau_2, \tau'). \quad (18)$$

For a steady or equilibrium system, it is more convenient to treat problems in the frequency domain,

$$G_{q\bar{q}}^{\sigma\sigma'}(\omega) = G_{q\bar{q}}^{0,\sigma\sigma'}(\omega) + \sum_{\sigma_1, \sigma_2} \sigma_1 \sigma_2 G_{q\bar{q}}^{0,\sigma\sigma_1}(\omega) \Sigma_{\bar{q}\bar{q}}^{\sigma_1\sigma_2}(\omega) G_{q\bar{q}}^{\sigma_2\sigma'}(\omega). \quad (19)$$

Feynman diagrams for phonon self-energy are the same as those in Ref. 22. Figure 1 shows some lowest-order Feynman diagrams. In the following we summarize the Feynman rules which are used to write the proper self-energy  $\Sigma_{\bar{q}\bar{q}}^{\sigma\sigma'}(\omega)$ . (1) Draw all topologically distinct Feynman diagrams for the proper self-energy with two terminals on the left and right separately. These diagrams should be connected and cannot be separated into two parts by cutting a single line. (2) Draw an arrow on each line from left to right and label it with new variable  $(q_i, \omega_i)$ . The line represents an unperturbed Green's function  $G_{q_i\bar{q}_i}^{0,\sigma_j\sigma'_j}(\omega_i)$ .  $\sigma_j, \sigma'_j = \pm 1$  are the variables of the vertices the line connects, which will be discussed below. The variables of the two terminals are both  $(q, \omega)$ . Using the relations between the six Green's functions,  $G_{q_i\bar{q}_i}^{0,\sigma_j\sigma'_j}(\omega_i)$  can be obtained from

$$G_{q_i\bar{q}_i}^{0,r}(\omega_i) = \lim_{\delta \rightarrow 0^+} [(\omega_i + i\delta)^2 - \omega_{q_i}^2]^{-1}. \quad (20)$$

(3) Label the vertices: each internal vertex with new variable  $\sigma_i$  ( $\sigma_i = \pm 1$ ), the two terminal vertices with  $\sigma$  on the left and  $\sigma'$  on the right. If only one terminal vertex exists, the self-energy is zero when  $\sigma \neq \sigma'$ . Each  $n$ -leg vertex contributes a factor  $F_{q_1\bar{q}_1, q_2\bar{q}_2, \dots, q_n\bar{q}_n}$ . Use  $\bar{q}_i$  in  $F$  if the line  $(q_i, \omega_i)$  goes into the vertex and use  $q_i$  in  $F$  if the line goes out of the vertex. The momentum conservation is automatically included in the factor. (4) At each vertex a factor of  $2\pi\delta(\sum_{i_{in}} \omega_{i_{in}} - \sum_{i_{out}} \omega_{i_{out}})$  is associated with energy conservation. The line  $(q_{i_{in}}, \omega_{i_{in}})$  enters the vertex and the line

$(q_{i_{out}}, \omega_{i_{out}})$  leaves the vertex. The two terminal vertices only contribute one energy conservation factor. (5) Multiply all the internal  $\sigma$  variables and a coefficient

$$c = (-1)^{1 + \sum_{n \geq 3} N_n} (i)^{2 + \sum_{n \geq 3} n + 2/2N_n} (\hbar)^{\sum_{n \geq 3} n - 2/2N_n} \prod_{n \geq 3} [(n-1)!]^{N_n} \frac{1}{S}, \quad (21)$$

where  $N_n$  is the number of  $n$ -leg vertices and  $S$  is the symmetry factor of the Feynman diagram. (6) The sums or integrations are performed over all the internal variables. For example, the self-energy of Fig. 1(c) is

$$\begin{aligned} \Sigma_{\bar{q}\bar{q}}^{\sigma\sigma'}(\omega) &= \sum_{q_1 \dots q_5} \sum_{\sigma_1} \int \frac{d\omega_1}{2\pi} \dots \int \frac{d\omega_5}{2\pi} (-54i\hbar^3) \\ &\times \sigma_1 2\pi \delta(\omega - \omega_1 - \omega_2 - \omega_3) \\ &\times 2\pi \delta(\omega_1 + \omega_2 - \omega_4 - \omega_5) \\ &\times F_{\bar{q}_1 q_1 q_2 q_3} F_{\bar{q}_1 \bar{q}_2 q_4 q_5} F_{\bar{q}_3 \bar{q}_4 \bar{q}_5 q} G_{q_1 \bar{q}_1}^{0,\sigma\sigma_1}(\omega_1) G_{q_2 \bar{q}_2}^{0,\sigma\sigma_1}(\omega_2) \\ &\times G_{q_3 \bar{q}_3}^{0,\sigma\sigma'}(\omega_3) G_{q_4 \bar{q}_4}^{0,\sigma_1\sigma'}(\omega_4) G_{q_5 \bar{q}_5}^{0,\sigma_1\sigma'}(\omega_5). \end{aligned} \quad (22)$$

The Feynman rules can be applied to calculate four types of self-energy:  $\Sigma^{++} = \Sigma^t$ ,  $\Sigma^{--} = \Sigma^t$ ,  $\Sigma^{+-} = \Sigma^<$ , and  $\Sigma^{-+} = \Sigma^>$ . The other two kinds of self-energy are  $\Sigma^r$  and  $\Sigma^a$ . They have similar relations between each other as the Green's functions and only one of them is independent in equilibrium.

#### E. Retarded self-energy and phonon lifetime

In the quasi-particle approximation, the phonon frequency  $\omega_q$  suffers a complex shift  $\Delta_q - i\Gamma_q$  due to phonon-phonon interactions, where  $\Gamma_q$  is the reciprocal phonon lifetime and  $2\Gamma_q$  is the full width at half maximum (FWHM) of the phonon peak in spectra. Then the frequency of the quasi-phonon is  $\tilde{\omega}_q = \omega_q + \Delta_q$ . The retarded phonon Green's function can be written as

$$G_{q\bar{q}}^r(\omega) = \frac{1}{\omega^2 - (\omega_q + \Delta_q - i\Gamma_q)^2}. \quad (23)$$

The Dyson equation for the retarded Green's function is

$$G_{q\bar{q}}^r(\omega) = \frac{1}{\omega^2 - \omega_q^2 - \Sigma_{\bar{q}\bar{q}}^r(\omega)}. \quad (24)$$

The quasi-particle approximation is valid if

$$|\Delta_q - i\Gamma_q| \ll \omega_q. \quad (25)$$

With this condition, from Eqs. (23) and (24) we get the relations

$$\text{Re}[\Sigma_{\bar{q}\bar{q}}^r(\omega_q)] \cong 2\omega_q \Delta_q, \quad (26)$$

$$\text{Im}[\Sigma_{\bar{q}\bar{q}}^r(\omega_q)] \cong -2\omega_q \Gamma_q = -\frac{2\omega_q}{\tau_q}. \quad (27)$$

The imaginary part of the retarded self-energy gives phonon lifetime. The condition of the quasi-particle approxima-

tion becomes  $|\Sigma_{\bar{q}q}^r(\omega_q)| \ll \omega_q^2$ . Note that  $\Sigma^r(-\omega) = [\Sigma^r(\omega)]^*$  implies  $\text{Re}[\Sigma^r(-\omega)] = \text{Re}[\Sigma^r(\omega)]$  and  $\text{Im}[\Sigma^r(-\omega)] = -\text{Im}[\Sigma^r(\omega)]$ . The retarded self-energy of “ $\omega$ -independent” diagrams is real. To study phonon lifetime, we only need to calculate “ $\omega$ -dependent” diagrams.

The NEGF formalism has advantage over the Matsubara formalism in the numerical calculation of the phonon lifetime when considering high order perturbations. In the Matsubara formalism, we have no choice but to calculate the self-energy of the Matsubara Green's function by diagrammatic techniques, then get the retarded self-energy through an analytical continuation. The situation is different in the NEGF formalism. There are four types of self-energy, which can be calculated by the Feynman rules, and the phonon lifetime can be directly taken from any one of the four self-energies. For example, the phonon lifetime can be expressed by the “lesser” self-energy as

$$\tau_q = -\frac{4\omega_q f(\omega_q)}{\text{Im}[\Sigma_{\bar{q}q}^<(\omega_q)]}, \quad (28)$$

where  $f$  is the Bose-Einstein distribution function. We could choose one kind of self-energy which is convenient for numerical calculation. It is noted that  $G^{0,<}(\omega)$  and  $G^{0,>}(\omega)$  are represented by the Dirac delta functions. Benefiting from the property of the Dirac delta functions, the more  $G^{0,<}(\omega)$  and  $G^{0,>}(\omega)$  are included in the chosen self-energy, the less frequency integrations of free Green's functions are needed to be done numerically. This helps us to get more accurate numerical results with less computation time, especially when high order perturbations are considered.

### F. Nonequilibrium Green's function method and Fermi's golden rule

Fermi's golden rule is widely used to calculate phonon lifetime in previous studies. What is the relation and difference between the NEGF method and Fermi's golden rule? This is the question to be answered in this subsection.

Let us consider three-phonon interaction at first. The lowest-order self-energy contributed by the three-phonon interaction is described by the Feynman diagram shown in Fig. 1(a). Using the above Feynman rules, we can write down the corresponding lesser self-energy as

$$\begin{aligned} \Sigma_{\bar{q}q}^<(\omega) &= \sum_{q_1 q_2} \int \frac{d\omega_1}{2\pi} \int \frac{d\omega_2}{2\pi} (2i\hbar) 2\pi \delta(\omega - \omega_1 - \omega_2) \\ &\times F_{\bar{q}q_1 q_2} F_{q\bar{q}_1 \bar{q}_2} G_{q_1 \bar{q}_1}^{0,<}(\omega_1) G_{q_2 \bar{q}_2}^{0,<}(\omega_2). \end{aligned} \quad (29)$$

The free lesser Green's function is

$$G_{\bar{q}q}^{0,<}(\omega) = \frac{-i\pi}{\omega_q} \{f(\omega_q) \delta(\omega - \omega_q) + [f(\omega_q) + 1] \delta(\omega + \omega_q)\}. \quad (30)$$

The imaginary part of retarded self-energy can be obtained through the relation

$$\text{Im}[\Sigma_{\bar{q}q}^<(\omega)] = 2f(\omega) \text{Im}[\Sigma_{\bar{q}q}^r(\omega)]. \quad (31)$$

Using Eq. (27), the reciprocal phonon lifetime can be expressed as

$$\begin{aligned} \Gamma_q &= \sum_{q_1 q_2} \frac{\pi\hbar}{4\omega_q \omega_{q_1} \omega_{q_2}} |F_{\bar{q}q_1 q_2}|^2 \{ [f(\omega_{q_1}) + f(\omega_{q_2}) + 1] \\ &\times [\delta(\omega - \omega_{q_1} - \omega_{q_2}) - \delta(\omega + \omega_{q_1} + \omega_{q_2})] \\ &+ [f(\omega_{q_1}) - f(\omega_{q_2})] [\delta(\omega + \omega_{q_1} - \omega_{q_2}) - \delta(\omega - \omega_{q_1} \\ &+ \omega_{q_2})] \}. \end{aligned} \quad (32)$$

On the other hand, we can use Fermi's golden rule to solve this problem and obtain the same result of reciprocal phonon lifetime, which is presented in Ref. 42. Fermi's golden rule is also equivalent to the lowest-order NEGF for more than three-phonon interaction. This conclusion can be proven in a similar procedure as above and it will not be elaborated here.

In summary, NEGF of lowest order is equivalent to Fermi's golden rule but the higher order terms of NEGF give additional corrections to it. The NEGF method provides a more comprehensive and systematic way than Fermi's golden rule in treating phonon-phonon interactions.

### G. Thermal transport from phonon mean-free path

Thermal conductance of a system at temperature  $T$  can be given by the Landauer formula as

$$\sigma = \frac{1}{L} \sum_{q(v_q^x > 0)} \hbar \omega_q v_q^x \frac{\partial f(\omega_q)}{\partial T} \Xi_q, \quad (33)$$

where  $L$  is the length of system in the direction of heat flow ( $x$  direction here),  $v_q^x$  is the phonon velocity in the  $x$  direction,  $f(\omega_q)$  is the Bose-Einstein distribution, and  $\Xi_q$  is the transmission function of phonon mode  $q \equiv (\mathbf{q}, j_q)$ . Equation (33) is valid from one dimensional (1D) to three dimensional (3D). Thermal conductivity has the form of  $\kappa = \sigma L/S$  in 3D systems, where  $S$  is the cross-section area. Moreover, for quasi-1D systems, we define  $\kappa = \sigma L$ .

A phenomenological formula is proposed to calculate phonon transmission function from the mean-free path.<sup>10,27,28</sup>

$$\Xi_q = (1 + L/l_q)^{-1}, \quad (34)$$

with  $l_q = v_q \tau_q$ . This formula is first proven for electron transmission function by Datta<sup>43</sup> and then for phonon transmission function by Yamamoto *et al.*<sup>44</sup> and Stoltz *et al.*<sup>45</sup> The premises of the phenomenological formula are that the concept of single-particle transmission function is valid and the transport is in the quasiballistic region. The formula can be used without problem when the phonon-phonon interactions are weak.

When  $L \ll l_q$ ,  $\Xi_q = 1$ , it corresponds to the ballistic limit; when  $L \gg l_q$ ,  $\Xi_q = l_q/L$ , thermal conductivity is

$$\kappa = \sum_{q(v_q^x > 0)} \hbar \omega_q \frac{1}{V} \frac{\partial f(\omega_q)}{\partial T} v_q^x l_q, \quad (35)$$

where  $V = L$  in 1D case and  $V = LS$  for 3D case. It reproduces the well-known Debye-Peierls formula for thermal transport.

The formula covers the range from ballistic to diffusive regime.<sup>10,27</sup>

### III. APPLICATIONS

We apply the general theory developed to study explicit models in this section. First we introduce two 1D atom chain models and investigate them by NEGF. Then a quasi-classical molecular-dynamics (QMD) method is applied to the same models and thermal conductances from both methods are compared. Finally calculated results and related discussion are provided.

#### A. One-dimensional atom chain models

The 1D atom chain models have been intensively studied. One of the remarkable problems is in what condition the thermal transport of a 1D system obeys Fourier law. The Fermi-Pasta-Ulam (FPU)  $\beta$  model and the  $\phi^4$  model are two example models which are extensively used due to their simplicity. It is found that the thermal conductivity in the FPU- $\beta$  model diverges with system size due to the momentum conservation while it is convergent in the  $\phi^4$  model.<sup>46–49</sup> Previous study indicates that the external potential plays a determinant role for normal thermal conduction.<sup>47,50</sup>

We will study the FPU- $\beta$  model and the  $\phi^4$  model with an additional harmonic on-site potential. In the following, these two models are denoted as models I and II, respectively. The Hamiltonian of model I is

$$H = \sum_i \left[ \frac{\dot{u}_i^2}{2} + \frac{K}{2}(u_i - u_{i+1})^2 + \frac{K_0}{2}u_i^2 + \frac{\beta}{4}(u_i - u_{i+1})^4 \right]. \quad (36)$$

The Hamiltonian of model II has the form

$$H = \sum_i \left[ \frac{\dot{u}_i^2}{2} + \frac{K}{2}(u_i - u_{i+1})^2 + \frac{K_0}{2}u_i^2 + \frac{\mu}{4}u_i^4 \right]. \quad (37)$$

They share the same harmonic Hamiltonian:

$$H_0 = \sum_i \left[ \frac{\dot{u}_i^2}{2} + \frac{K}{2}(u_i - u_{i+1})^2 + \frac{K_0}{2}u_i^2 \right]. \quad (38)$$

The dispersion relation of unperturbed phonon can be expressed as  $\omega_q = \sqrt{K_0 + 2K(1 - \cos qa)}$ . We set the lattice constant  $a = 1 \text{ \AA}$ ,  $K = 1.0 \text{ eV}/(\text{amu} \text{ \AA}^2)$ , and  $K_0 = 0.1K$ . These parameters are chosen to be the same as those in Ref. 16, where model II is studied by the QMD method. The group velocity is defined as  $v_q = \partial\omega_q / \partial q$ . Since a harmonic on-site potential is included in  $H_0$ ,  $v_{q=0} = 0$  and  $\omega_q$  ranges from  $0.31 \times 10^{14}$  to  $1.99 \times 10^{14} \text{ s}^{-1}$ .

For model I, we choose  $\beta = 1.0 \text{ eV}/(\text{amu}^2 \text{ \AA}^4)$  and the NEGF method provides converged result until  $T = 600 \text{ K}$ . For model II,  $\mu = 1.0 \text{ eV}/(\text{amu}^2 \text{ \AA}^4)$  is also tried but the NEGF method fails even for  $T = 100 \text{ K}$ . To get a converged result, we select  $\mu = 0.05 \text{ eV}/(\text{amu}^2 \text{ \AA}^4)$  and the NEGF method would still work at the temperature higher than 1000 K. This is partially because a small anharmonic parameter  $\mu$  is chosen. The calculations indicate that the NEGF method

which is based on perturbation expansion is only suitable for weak phonon-phonon interactions.

The two models share the same set of Feynman diagrams for self-energy. Since their anharmonic parts are both quartic, only those vertices with four legs will appear in the Feynman diagrams. The four-leg vertex of model I has the form of

$$F_{q_1 q_2 q_3 q_4} = \Delta(q_1 + q_2 + q_3 + q_4) \frac{2\beta}{N} [1 - \cos q_2 a - \cos q_3 a - \cos q_4 a + \cos(q_2 + q_3)a + \cos(q_2 + q_4)a + \cos(q_3 + q_4)a - \cos(q_2 + q_3 + q_4)a]. \quad (39)$$

As  $q_i$  ( $i = 1, 2, 3, 4$ ) approaches zero,  $F_{q_1 q_2 q_3 q_4}$  goes zero. The four-leg vertex of model II is

$$F_{q_1 q_2 q_3 q_4} = \Delta(q_1 + q_2 + q_3 + q_4) \frac{\mu}{N}. \quad (40)$$

Only  $\omega$ -dependent diagrams of lowest orders are considered in our calculation. These include one diagram of  $O(\lambda^4)$  [Fig. 1(b)] and two diagrams of  $O(\lambda^6)$  [Figs. 1(c) and 1(d)]. Using the Feynman rules developed above, the analytical form of self-energy for these three diagrams can be derived and then be used in numerical calculation. As described in the previous section, phonon lifetime and mean-free path can be obtained from the imaginary part of the retarded self-energy. Thermal transport properties can be given by the Landauer formula.

#### B. Comparison of thermal conductance from nonequilibrium Green's function and quasiclassical molecular dynamics

Based on a generalized Langevin dynamics, the QMD method is developed to study quantum thermal transport in Ref. 16, where the considered system consists of a central junction part and two leads serving as heat baths. This method uses quantum heat baths derived from Bose-Einstein statistics and treats the central part classically. In Ref. 16, it is proven that the method can produce correct results both in quantum ballistic and classical diffusive limits.

The QMD method is employed to give thermal conductances of the two models.  $3 \times 10^8$  MD steps are used in the calculation with the time step of  $10^{-16} \text{ s}$ . The comparison of thermal conductance with that from the NEGF method is presented in Fig. 2 for models I and II. Both methods give essentially the same results at low temperatures. Deviations appear at high temperatures. The NEGF method gives larger thermal conductance for model I and smaller thermal conductance for model II. It is not unexpected that they give quantitatively different results. A quasiclassical approximation is made in the QMD method. The NEGF method makes perturbation expansion and neglects higher order terms which become important at high temperatures. Both methods provide only approximate results, and it is still unclear which method is superior. More work is needed to understand these differences.

#### C. Results and discussion

The results of models I and II are presented in Figs. 3 and 4, respectively. The mode-dependent phonon lifetime at dif-

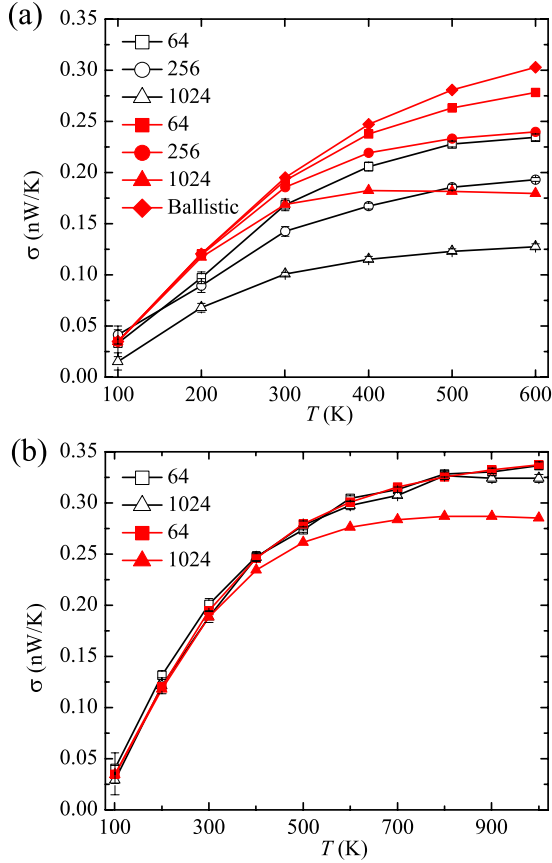


FIG. 2. (Color online) Comparison of thermal conductance ( $\sigma$ ) from different methods: NEGF (red solid symbols) and QMD (black open symbols). (a) Thermal conductance of model I with the system size  $N=64, 256,$  and  $1024$ . Ballistic thermal conductance is also provided by NEGF. (b) Thermal conductance of model II with the system size  $N=64$  and  $1024$ .

ferent temperatures and the temperature-dependent thermal conductivity with different system sizes are shown.

The two models with different types of anharmonic potentials give distinct properties of phonon lifetime. For model I, the translational invariant quartic potential leads to zero retarded self-energy and infinite phonon lifetime for infinite long-wavelength mode, which is not shown in Fig. 3(a). Long wavelength phonon mode has long lifetime. In contrast, the long-wavelength phonon of model II, which experiences large scattering due to the existence of quartic on-site potential, has short lifetime.

Increasing temperature has two effects on thermal conductivity: shorter phonon mean-free path and more phonon excitation. The first effect decreases and the second effect increases thermal conductivity. When the system length is much smaller than the phonon mean-free path, the first effect has minor influence and thermal conductivity would increase with increasing temperature. At high temperatures, for a system whose length is comparable to the phonon mean-free path, the excitation of phonon modes becomes less important to thermal transport and then thermal conductivity would decrease with increasing temperature due to the shortening of phonon mean-free path. These are verified in Figs. 3(b) and 4(b). For very large system at low temperatures, the thermal

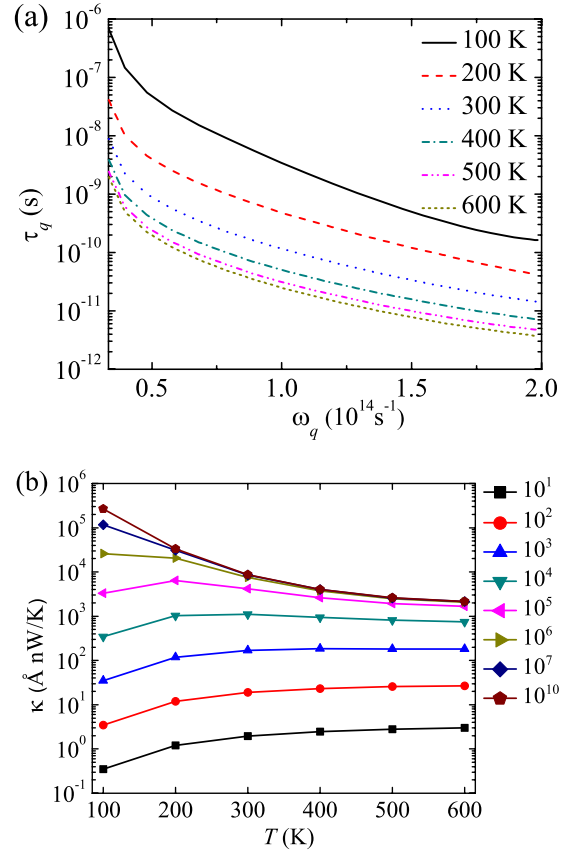


FIG. 3. (Color online) Results of model I. (a) Phonon lifetime  $\tau_q$  at  $T=100\text{--}600$  K. The nearly infinite lifetimes of very long-wavelength phonons are not presented in the figure. (b) Thermal conductivity  $\kappa$  with the system size  $N=10^1, 10^2, 10^3, 10^4, 10^5, 10^6, 10^7, 10^{10}$  at  $T=100\text{--}600$  K.

conductivity of model I decreases as the temperature increases, which is different from that of model II. This may be explained by the fact that the temperature has larger influence on the phonon mean-free path in model I than in model II at low temperatures.

One of the advantages of our method is that once the mode-dependent phonon mean-free path is obtained, thermal conductivity of different system sizes can be obtained easily. It would be interesting to show the size-dependent behavior of thermal conductivity, which is presented in Fig. 5. When the system length is much smaller than the phonon mean-free path (i.e., the ballistic regime) thermal conductance does not change with system size, and thermal conductivity increases linearly with the system size. When the system length increases to much larger than the phonon mean-free path (of order of  $10^6 \text{ \AA}$  in model II at 100 K) (i.e., the diffusive regime), thermal conductivity will cease to change with system size. A ballistic-diffusive transition with increasing system size is shown in Fig. 5 clearly.

The FPU- $\beta$  model, model I with  $K_0=0$ , is widely known to have divergent thermal conductivity. With an additional harmonic on-site potential, we get a finite bulk-limit thermal conductivity for model I as shown in Fig. 5. How does a nonzero  $K_0$ , the harmonic on-site potential, induce different behavior of thermal conductivity? An analysis on long-

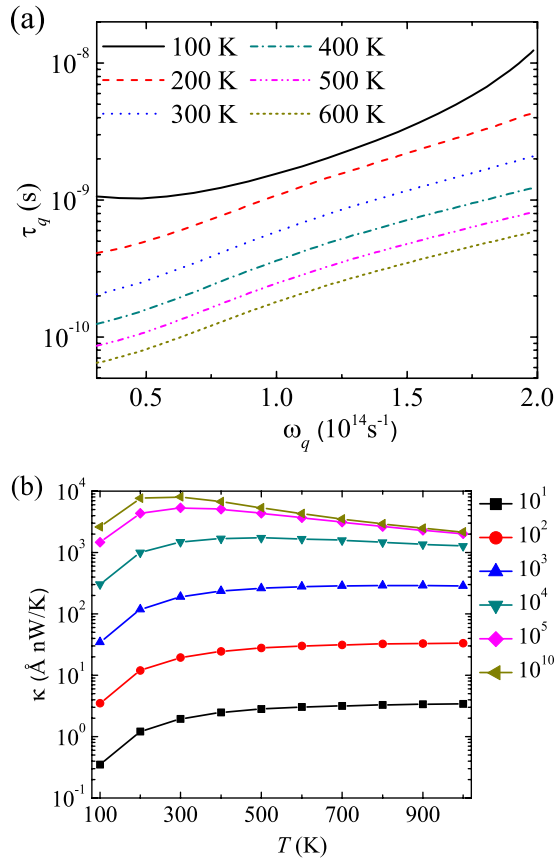


FIG. 4. (Color online) Results of model II. (a) Phonon lifetime  $\tau_q$  at  $T=100\text{--}600$  K. (b) Thermal conductivity  $\kappa$  with the system size  $N=10^1, 10^2, 10^3, 10^4, 10^5, 10^{10}$  at  $T=100\text{--}1000$  K.

wavelength phonon modes will answer this question. As  $q$  approaches zero,  $F_{qq;qq} \propto q$  and  $\Sigma_{qq}^r(\omega_q) \propto q^2$ . When  $K_0=0$ ,  $\omega_q \propto q$ ,  $v_q \rightarrow \text{constant}$ ,  $\tau_q \propto q^{-1}$ , and  $l_q \propto q^{-1}$ . Thermal conductivity contributed by long-wavelength phonon modes would diverge with increasing system size. When  $K_0 \neq 0$ ,  $\omega_q \rightarrow \text{constant}$ ,  $v_q \propto q$ ,  $\tau_q \propto q^{-2}$ , and  $l_q \propto q^{-1}$ . The quadratic on-site potential breaks translational invariance and the phonon modes with very long wavelength have nearly zero group velocity. Although those phonon modes has nearly infinite mean-free path, it can be shown analytically that the thermal conductivity contributed by them does not diverge with increasing system size for  $K_0 \neq 0$ . Other phonon modes which have finite mean-free paths also contribute a finite thermal conductivity. As such, finite thermal conductivity is obtained in bulk limit for model I.

Comparing the results of the two models may give some information on how an anharmonic on-site potential influences thermal transport. A quartic on-site potential is included in model II. The anharmonic parameter  $\mu$  of model II is 20 times as small as that of model I. However, model II gives much shorter phonon lifetime for low-frequency modes, which are very important for thermal transport especially at low temperatures. As shown in Fig. 5, the bulk-limit thermal conductivity of model II is much smaller than that of model I at 100 K. The comparison indicates that even a small quartic on-site potential can largely decrease the phonon lifetimes of long-wavelength modes and significantly affect ther-

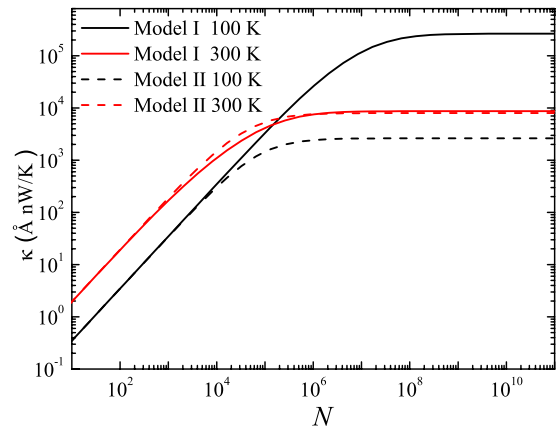


FIG. 5. (Color online) Thermal conductivity  $\kappa$  of different system sizes for models I and II at  $T=100$  and 300 K.

mal transport especially at low temperatures. Our results confirm that the external potential plays a determinant role in thermal transport.

#### IV. SUMMARY

We have provided an approach in studying phonon-phonon interactions and ballistic-diffusive thermal transport by the NEGF method and the Landauer formula. A formalism of NEGF has been developed to systematically study phonon-phonon interactions in momentum space at finite temperatures in equilibrium. Using a phenomenological transmission function, which can be obtained from the mode-dependent phonon mean-free path given by the NEGF formalism, the Landauer formula predicts thermal transport properties from ballistic to diffusive region. Our approach is efficient for investigating ballistic-diffusive thermal transport in weak-interaction situations, where little additional computational effort is needed when the system size changes. As an application, we have investigated two 1D atom chain models. The results obtained are qualitatively in agreement with those by the QMD method. It is found that an additional harmonic on-site potential in the FPU- $\beta$  model could remove the divergence of thermal conductivity and a small quartic on-site potential can largely reduce the phonon lifetimes of long-wavelength modes. The results confirm that the external potential plays an important role in thermal transport.<sup>47,50</sup>

#### ACKNOWLEDGMENTS

The authors are grateful to Gang Zhang, Jingtao Lü, Lifa Zhang, and Xiang Wu for discussions. This work is supported by an endowment fund Grant No. R-144-000-222-646 from NUS, the National Natural Science Foundation of China (Grant No. 10547002), and the Ministry of Science and Technology of China (Grants No. 2006CB605105 and No. 2006CB0L0601). J.S.W. is supported in part by an NUS Faculty Research Grant No. R-144-000-173-101/112.



\*Corresponding author; dwh@phys.tsinghua.edu.cn

- <sup>1</sup>D. G. Cahill, W. K. Ford, K. E. Goodson, G. D. Mahan, A. Majumdar, H. J. Maris, R. Merlin, and S. R. Phillpot, *J. Appl. Phys.* **93**, 793 (2003).
- <sup>2</sup>K. Schwab, E. A. Henriksen, J. M. Worlock, and M. L. Roukes, *Nature (London)* **404**, 974 (2000).
- <sup>3</sup>D. Li, Y. Wu, R. Fan, P. Yang, and A. Majumdar, *Appl. Phys. Lett.* **83**, 3186 (2003).
- <sup>4</sup>L. Shi, D. Li, C. Yu, W. Jang, D. Kim, Z. Yao, P. Kim, and A. Majumdar, *ASME J. Heat Transfer* **125**, 881 (2003).
- <sup>5</sup>J. Hone, M. Whitney, C. Piskoti, and A. Zettl, *Phys. Rev. B* **59**, R2514 (1999); P. Kim, L. Shi, A. Majumdar, and P. L. McEuen, *Phys. Rev. Lett.* **87**, 215502 (2001); M. Fujii, X. Zhang, H. Xie, H. Ago, K. Takahashi, T. Ikuta, H. Abe, and T. Shimizu, *ibid.* **95**, 065502 (2005); E. Pop, D. Mann, Q. Wang, K. E. Goodson, and H. Dai, *Nano Lett.* **6**, 96 (2006).
- <sup>6</sup>L. G. C. Rego and G. Kirzenow, *Phys. Rev. Lett.* **81**, 232 (1998).
- <sup>7</sup>T. Yamamoto, S. Watanabe, and K. Watanabe, *Phys. Rev. Lett.* **92**, 075502 (2004).
- <sup>8</sup>N. Mingo and D. A. Broido, *Phys. Rev. Lett.* **95**, 096105 (2005).
- <sup>9</sup>K. Saito, J. Nakamura, and A. Natori, *Phys. Rev. B* **76**, 115409 (2007).
- <sup>10</sup>J.-S. Wang, J. Wang, and J. T. Lü, *Eur. Phys. J. B* **62**, 381 (2008).
- <sup>11</sup>S. Lepri, R. Livi, and A. Politi, *Phys. Rep.* **377**, 1 (2003).
- <sup>12</sup>G. Zhang and B. Li, *J. Chem. Phys.* **123**, 114714 (2005).
- <sup>13</sup>L. H. Liang and B. Li, *Phys. Rev. B* **73**, 153303 (2006).
- <sup>14</sup>G. Fagas, A. G. Kozorezov, C. J. Lambert, J. K. Wigmore, A. Peacock, A. Poelaert, and R. den Hartog, *Phys. Rev. B* **60**, 6459 (1999).
- <sup>15</sup>A. Kambili, G. Fagas, V. I. Fal'ko, and C. J. Lambert, *Phys. Rev. B* **60**, 15593 (1999).
- <sup>16</sup>J.-S. Wang, *Phys. Rev. Lett.* **99**, 160601 (2007).
- <sup>17</sup>N. Mingo and L. Yang, *Phys. Rev. B* **68**, 245406 (2003).
- <sup>18</sup>T. Yamamoto and K. Watanabe, *Phys. Rev. Lett.* **96**, 255503 (2006).
- <sup>19</sup>A. Dhar and D. Sen, *Phys. Rev. B* **73**, 085119 (2006).
- <sup>20</sup>J.-S. Wang, J. Wang, and N. Zeng, *Phys. Rev. B* **74**, 033408 (2006).
- <sup>21</sup>N. Mingo, *Phys. Rev. B* **74**, 125402 (2006).
- <sup>22</sup>J.-S. Wang, N. Zeng, J. Wang, and C. K. Gan, *Phys. Rev. E* **75**, 061128 (2007).
- <sup>23</sup>T. Matsubara, *Prog. Theor. Phys.* **14**, 351 (1955).
- <sup>24</sup>N. Li, P. Tong, and B. Li, *Europhys. Lett.* **75**, 49 (2006).
- <sup>25</sup>N. Li and B. Li, *Europhys. Lett.* **78**, 34001 (2007).
- <sup>26</sup>N. Li and B. Li, *Phys. Rev. E* **76**, 011108 (2007).
- <sup>27</sup>J. Wang and J.-S. Wang, *Appl. Phys. Lett.* **88**, 111909 (2006).
- <sup>28</sup>P. G. Murphy and J. E. Moore, *Phys. Rev. B* **76**, 155313 (2007).
- <sup>29</sup>A. A. Maradudin and A. E. Fein, *Phys. Rev.* **128**, 2589 (1962).
- <sup>30</sup>M. Roufosse and P. G. Klemens, *Phys. Rev. B* **7**, 5379 (1973).
- <sup>31</sup>S. P. Hepplestone and G. P. Srivastava, *Phys. Rev. B* **74**, 165420 (2006).
- <sup>32</sup>Y. Gu and Y. Chen, *Phys. Rev. B* **76**, 134110 (2007).
- <sup>33</sup>K. N. Pathak, *Phys. Rev.* **139**, A1569 (1965).
- <sup>34</sup>I. P. Ipatova, A. A. Maradudin, and R. F. Wallis, *Phys. Rev.* **155**, 882 (1967).
- <sup>35</sup>M. R. Monga and K. N. Pathak, *Phys. Rev. B* **18**, 5859 (1978).
- <sup>36</sup>R. G. DellaValle and P. Procacci, *Phys. Rev. B* **46**, 6141 (1992).
- <sup>37</sup>P. Procacci, G. F. Signorini, and R. G. DellaValle, *Phys. Rev. B* **47**, 11124 (1993).
- <sup>38</sup>A. A. Abrikosov, L. P. Gorkov, and I. E. Dzyaloshinski, *Quantum Field Theoretical Methods in Statistical Physics* (Pergamon Press, New York, 1965).
- <sup>39</sup>H. Haug and A. P. Jauho, *Quantum Kinetics in Transport and Optics of Semiconductors* (Springer, Berlin, 1996).
- <sup>40</sup>M. Wagner, *Phys. Rev. B* **44**, 6104 (1991).
- <sup>41</sup>L. V. Keldysh, *Sov. Phys. JETP* **20**, 1018 (1965).
- <sup>42</sup>O. Madelung, *Introduction to Solid-State Theory* (Springer-Verlag, Berlin, Heidelberg, 1978).
- <sup>43</sup>S. Datta, *Electronic Transport in Mesoscopic Systems* (Cambridge University Press, Cambridge, 1995).
- <sup>44</sup>T. Yamamoto, K. Watanabe, and S. Watanabe, in *Oxford Handbook of Nanoscience and Technology: Frontiers and Advances*, edited by A. Narlikar and Y. Fu (Oxford University Press, New York, in press), Chap. 14.
- <sup>45</sup>G. Stoltz, M. Lazzeri, and F. Mauri, arXiv:0810.1830 (unpublished).
- <sup>46</sup>S. Lepri, R. Livi, and A. Politi, *Phys. Rev. Lett.* **78**, 1896 (1997).
- <sup>47</sup>B. Hu, B. Li, and H. Zhao, *Phys. Rev. E* **61**, 3828 (2000).
- <sup>48</sup>K. Aoki and D. Kusnezov, *Phys. Lett. A* **265**, 250 (2000).
- <sup>49</sup>K. Aoki and D. Kusnezov, *Phys. Rev. Lett.* **86**, 4029 (2001).
- <sup>50</sup>B. Hu, B. Li, and H. Zhao, *Phys. Rev. E* **57**, 2992 (1998).